

Poly(di-*n*-alkylsiloxane)s with Long Alkyl Side Groups

G. J. J. Out, A. A. Turetskii, and M. Möller\*,†

Department of Chemical Technology, University of Twente, P.O. Box 217,  
7500 AE Enschede, The Netherlands

D. Oelfin

Institut für Makromolekulare Chemie, Hermann-Staudinger-Haus, Albert Ludwigs-  
Universität, Stefan-Meier-Strasse 31, D-79104 Freiburg, Germany

Received October 15, 1993; Revised Manuscript Received February 15, 1994\*

**ABSTRACT:** High molecular weight samples of poly(di-*n*-pentylsiloxane) (PDPeS), poly(di-*n*-hexylsiloxane) (PDHS), and poly(di-*n*-decylsiloxane) (PDDES) have been prepared by means of anionic (PDPeS, PDHS) and cationic (PDDES) ring-opening polymerization of the corresponding hexa-*n*-alkylcyclotrisiloxanes. The phase behavior of the polymers has been studied by polarizing microscopy, differential scanning calorimetry, wide-angle X-ray scattering, and <sup>29</sup>Si solid-state NMR spectroscopy. Like the homologues with shorter alkyl substituents, all three new polysiloxanes showed two disordering transitions and formed a conformationally disordered mesophase before isotropization. Elongation of the alkyl side groups from ethyl to *n*-hexyl improved the stability of the hexagonal columnar mesophase, which is reflected in an increase in the mesophase temperature interval from  $\Delta T = 43$  °C for poly(diethylsiloxane) (PDES) to more than 310 °C in the case of PDHS. Optical polarizing microscopy indicated the formation of extended chain lamellae within this state. When the alkyl side groups were elongated to *n*-decyl, however, the conformationally disordered state was only observed by temperature-dependent <sup>29</sup>Si chemical shift anisotropy measurements as an undercooled phase in coexistence with the high-temperature crystalline phase.

## Introduction

Linear flexible chain molecules like poly(di-*n*-alkylsiloxane)s<sup>1-5</sup> [(R<sub>2</sub>SiO)<sub>*n*</sub>], poly(di-*n*-alkylsilylene)s<sup>6-8</sup> [(R<sub>2</sub>-Si)<sub>*n*</sub>], and poly(di-*n*-alkoxyphosphazene)s<sup>9,10</sup> [(RO)<sub>2</sub>PN]<sub>*n*</sub> share the feature of showing columnar mesophase behavior despite the absence of any classical mesogens in the molecular structure. Although poly(di-*n*-alkylsiloxane)s and poly(di-*n*-alkylsilylene)s clearly differ in main-chain flexibility, unusual chain stiffening is not reflected in values of the characteristic ratio  $C_{\infty}$ .<sup>11-13</sup> Apart from being able to form remarkably thick lamellar crystals,<sup>3,5,7,14</sup> these materials also crystallize as chain-folded lamellar crystals with thicknesses ranging between 5 and 20 nm.<sup>15,16</sup> It has been proposed that the origin of this mesophase behavior lies in the inherent incompatibility between the inorganic backbone and organic side groups, resulting in self-organization of the polymer chains into a columnar structure.<sup>17</sup> However, similar hexagonal columnar mesophases are also formed by apolar flexible chain molecules like anabarc polyethylene, poly(tetrafluoroethylene), poly(*p*-xylylene), and 1,4-*trans*-polybutadiene.<sup>18-22</sup> Therefore, it must be assumed that the presence of high main-chain flexibility rather than the existence of repulsive intramolecular interactions is essential for macromolecules in order to show this kind of mesophase behavior. Nevertheless, the side groups appear to be of great importance for the stability of the columnar mesophase. This is clearly illustrated by the fact that at normal pressure the lowest homologue of the series of poly(di-*n*-alkylsiloxanes), i.e., poly(dimethylsiloxane), does not show mesophase behavior despite high main-chain flexibility.

In order to study the influence of the alkyl side group length on the mesophase behavior of poly(di-*n*-alkylsiloxane)s, a series of new poly(di-*n*-alkylsiloxane)

**Table 1. Molecular Weights, MWDs, Intrinsic Viscosities, and Mark-Houwink Parameters of PDPeS, PDHS, and PDDES As Determined in Toluene**

polymer	$M_w^a$	$M_w/M_n^a$	$[\eta]^b$ (dL/g)	$[\eta]^a$ (dL/g)	$\alpha^a$	log $K^a$
PDPeS	660 000	2.0	1.23	1.28	0.514	-2.850
PDHS	1 333 000	1.8	1.93	1.83	0.463	-2.560
PDDES	905 000	1.5	1.22	1.21	0.452	-2.598

<sup>a</sup> From GPC according to universal calibration. <sup>b</sup> From viscosity measurements using an Ubbelohde (298 K).

homopolymers has been synthesized with alkyl side groups containing 5, 6, and 10 carbon atoms and their thermal behavior will be compared with that of the corresponding polymers substituted with ethyl, *n*-propyl, and *n*-butyl side groups, i.e., poly(diethylsiloxane) (PDES),<sup>1-5</sup> poly(di-*n*-propylsiloxane) (PDPS),<sup>1,3,4,23</sup> and poly(di-*n*-butylsiloxane) (PDBS).<sup>4,23</sup>

For the sake of clarity, it might be helpful to define the classification which will be used in this work to describe the phase behavior of the investigated poly(di-*n*-alkylsiloxane)s at the example of PDES. The conformationally disordered state below the isotropization temperature ( $\alpha_m$  or  $\mu$ -phase<sup>3-5</sup>) is denoted as the hexagonal columnar (LC) state. All ordered states found at lower temperatures will be referred to as crystalline states.

## Experimental Section

**GPC.** GPC measurements have been carried out with toluene as a solvent, using Waters  $\mu$ -Styragel columns (pore size 10<sup>5</sup>, 10<sup>4</sup>, 10<sup>3</sup>, and 10<sup>6</sup> Å). Molecular weights were determined by universal calibration based on narrowly distributed polystyrene standards.<sup>24,25</sup> A dual detection system consisting of a differential refractometer (Waters Model 410) and a differential viscometer (Viscotek Model H502, UNICAL software) allowed simultaneous determination of molecular weights, molecular weight distributions, intrinsic viscosities  $[\eta]$ , and Mark-Houwink parameters  $K$  and  $\alpha$  (Table 1).

**Calorimetry.** A Perkin-Elmer DSC-7 equipped with a PE-7700 computer and TAS-7 software was used to monitor the thermal transitions at scan rates between 0.5 and 20 K/min.

\* To whom correspondence should be sent.

† Present address: Organische Chemie III, Makromolekulare Chemie, Universität Ulm, D-89069 Ulm, Germany.

\* Abstract published in *Advance ACS Abstracts*, April 15, 1994.

Sample weights were typically chosen between 2 and 5 mg. Transition entropies were calculated assuming equilibrium, i.e.,  $\Delta H = T\Delta S$ . Cyclohexane was used as the calibration standard. The onset of the recorded endotherm on heating was taken as the transition temperature.

**Optical Microscopy.** Optical polarizing microscopy was performed using a Leitz Ortholux II Pol BK microscope equipped with a Mettler FP 82 hot stage.

**NMR.** High-resolution solid-state  $^{29}\text{Si}$ -NMR measurements were carried out as described before on a Bruker CXP 300 spectrometer at 59.63 MHz.<sup>5</sup> MAS spectra were recorded by spinning the sample at 2–3 kHz around an axis at 54.7° toward  $H_0$  and applying high-power proton decoupling. CSA spectra were recorded under the same conditions without rotation around the magic angle. Cross polarization (CP) was applied only for low-temperature spectra. High-power decoupled spectra (DD) of the materials in the dynamically disordered states at higher temperatures were recorded with delay times between individual scans, which allowed near to complete  $T_1$  relaxation. Temperatures were monitored using a thermocouple which was located near the spinning rotor. Due to variations in the gas stream monitored temperatures showed deviations from the actual sample temperatures as indicated in the figure captions.

**X-ray Diffraction.** X-ray diffraction patterns have been recorded using Ni-filtered Cu K $\alpha$  radiation. Temperature-dependent diffractograms have been recorded on a circular film with a radius of 57.3 mm, using a Guinier–Simon camera. In order to detect the scattering intensity at scattering angles as low as 1.5° (2 $\theta$ ), a slight adjustment of the beam stop has been made. The samples were cooled by means of a constant flow of cold nitrogen gas, and the temperature was controlled by means of a thermocouple introduced into the nozzle in the direct vicinity of the specimen. The temperature variation in the sample compartment was checked with an additional thermocouple and was found to be  $\pm 2$  K. Prior to measurements, the sample was cooled at a rate of 5 K/min to 193 K and then heated at a rate of 5 K/min to the required temperature, followed by annealing for 30 min. Exposure times were approximately 3 h. Optical density data were collected from the photographically obtained patterns using a linear microdensitometer LS20 (Delft Instruments) controlled by SCANPI software.

## Results and Discussion

**Synthesis.** Hexa-*n*-alkylcyclotrisiloxanes have been synthesized by condensation of di-*n*-alkyldichlorosilanes with ZnO as described before.<sup>26</sup> Distillation of the crude condensation product gave the cyclic trimer in 45% yield with purities ranging between 93 and 98%. Synthesis of di-*n*-alkyldichlorosilanes has been accomplished by hydrosilylation of the corresponding 1-alkenes with dichlorosilane ( $\text{H}_2\text{SiCl}_2$ ) in the presence of  $\text{H}_2\text{PtCl}_6$ . Typically, yields of 80–85% of the di-*n*-alkyldichlorosilane were obtained.<sup>27</sup>

Polymer synthesis has been carried out either by anionic ring-opening polymerization (PDPeS, PDHS) under high-vacuum conditions using CsOH as initiator or by cationic ring-opening polymerization (PDDS), which was performed under argon using  $\text{CF}_3\text{SO}_3\text{H}$  as an initiating system. In the case of anionic ring-opening polymerization, it was observed that longer alkyl side groups required progressively longer polymerization times and led to an earlier onset of redistribution reactions in relation to the degree of conversion. Anionic polymerization of hexa-*n*-decylcyclotrisiloxane resulted in a yield of 18% of relatively low molecular weight material ( $M_w = 36\,000$ ,  $\text{DP} = 110$ ), presumably due to concomitant occurrence of redistribution reactions. High molecular weight material could only be obtained by using cationic polymerization. Yields of PDPeS, PDHS, and PDDS were on the order of 70%. Molecular weights, polydispersity index and intrinsic viscosities (in toluene) of fractionated samples are summarized in Table 1. Further details regarding the synthesis of monomers and polymers will be published elsewhere.<sup>28</sup>

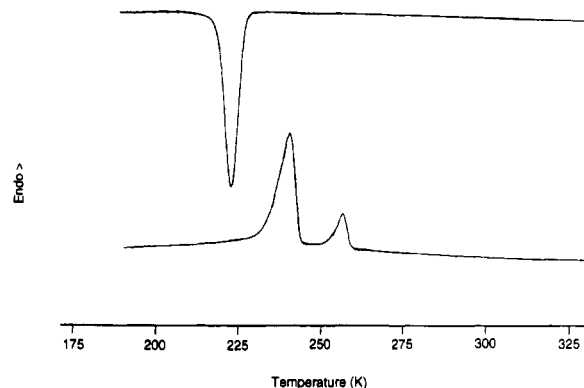


**Figure 1.** DSC heating and cooling scan of poly(di-*n*-pentylsiloxane) (rate 5 K/min).

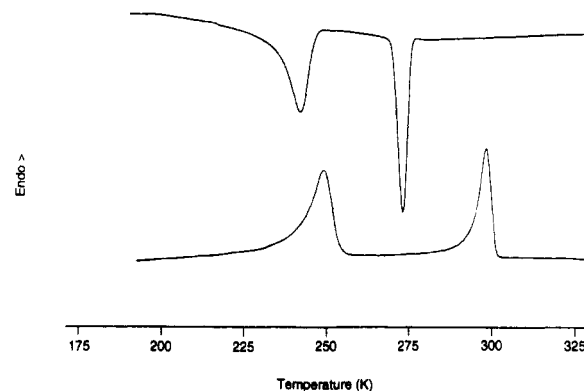


**Figure 2.** DSC heating and cooling scan of poly(di-*n*-hexylsiloxane) (rate 5 K/min).

**DSC.** Calorimetric studies on a PDPeS sample, which had been cooled at a rate of 5 K/min from room temperature to 193 K and annealed at this temperature for 10 min, revealed the existence of two solid-state disordering transitions at 231 and 251 K respectively (Figure 1). Although it is not indicated in Figure 1, a recrystallization transition was observed at 491 K in the first heating scan, which was absent in subsequent heating scans. No further transition was observed, but by means of optical polarizing microscopy, it was found that, above the upper disordering transition, the material remained strongly birefringent until isotropization occurred at 603 K. This final transition took place gradually within a temperature range of 20 K and was reversible. The reversibility proved that loss of birefringence was not due to thermal degradation of the sample. As will be discussed below, the birefringent state above the two disordering transitions observed in the DSC thermogram can be assigned to the formation of a hexagonal columnar phase.

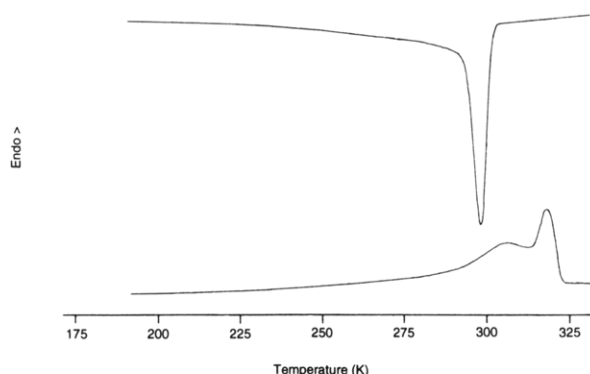
Heating a sample of PDHS, which had been cooled from room temperature to 193 K at a rate of 5 K/min and which was consecutively annealed at that temperature for 10 min, yielded two solid–solid phase transitions at 246 and 296 K, respectively (Figure 2). Like in the case of PDPeS a recrystallization transition occurred at 493 K in the first heating scan, which was absent in subsequent heating scans. Also in this case, it was not possible to observe the reversible isotropization transition by DSC, which was evident in optical polarizing microscopy studies by the loss of birefringence between 583 and 603 K. Annealing at 583 K resulted in reappearance of birefringence, demonstrating the reversibility of the transition.

When a sample of PDDS, which had been cooled from 393 to 193 K at a rate of 5 K/min, was studied by DSC, two transitions could be observed upon heating at 286 and 313 K, respectively. Independent of the annealing pro-

**Table 2. Thermal Transitions of Poly(di-*n*-alkylsiloxane)s As Observed on Heating at a Rate of 5 K/min**

polymer	DP <sup>a</sup>	<i>T<sub>g</sub></i> (K)	<i>T<sub>d1</sub></i> (K)	$\Delta H_{d1}$ (kJ/mol)	$\Delta S_{d1}$ (J/K·mol)	<i>T<sub>d2</sub></i> (K)	$\Delta H_{d2}$ (kJ/mol)	$\Delta S_{d2}$ (J/K·mol)	<i>T<sub>i</sub></i> (K)
PDES	1760	135	207	2.7	13.2	283	1.8	6.5	326
PDPS	1310	163	222	3.0	13.4	343	2.2	6.4	479
PDBS	2013	157	229	3.6	15.7	254	0.9	3.5	583 <sup>b</sup>
PDPeS	3535	167	231	9.0	38.8	251	1.9	7.6	603 <sup>b</sup>
PDHS	6030		246	6.7	27.2	296	5.1	17.2	603 <sup>b</sup>
PDDS	2750		286	21 <sup>c</sup>	72 <sup>c</sup>	313	9 <sup>c</sup>	29 <sup>c</sup>	

<sup>a</sup> Based on  $M_w$  as determined by GPC. <sup>b</sup> Disappearance of birefringence. <sup>c</sup> Estimated value based on graphic evaluation of the thermal transitions in the DSC heating scan.

**Figure 3.** DSC heating and cooling scan of poly(di-*n*-decylsiloxane) (rate 5 K/min).

cedure, the first transition was very broad (Figure 3). Significant hysteresis was observed upon cooling for both transitions, whereby the lower one broadened to an extent that it was barely recognized.

Table 2 summarizes the thermal behavior of the different poly(di-*n*-alkylsiloxanes) which have been investigated so far.<sup>1-5,23,29,30</sup>

**The  $\mu$ -Phase.** Examination of the birefringent textures of PDPeS and PDHS by polarizing microscopy showed that, upon slow cooling of the isotropic melt, band-shaped structures were formed. The length and to a much smaller extent also the thickness of these bands increased with decreasing temperature (Figure 4a). Further cooling to a temperature just above the upper disordering transition observed by DSC resulted in the formation of a focal-conic fan texture which is regarded as characteristic for a columnar or smectic ordering of the polymer chains (Figure 4b). This focal-conic fan texture was less evident in the case of PDHS, in which case the texture of the material was still composed of broad band-shaped crystallites at a temperature just above the second disordering transition (Figure 5a,b). Based on reflection and transmission optical microscopy observations, previous studies on mesomorphic PDES had revealed that the bands are to be considered as the lateral faces of lamellar domains with an average thickness of 1.5–2  $\mu\text{m}$ .<sup>14</sup> Comparison of optical micrographs with TEM micrographs confirmed the formation of unusually thick lamellar structures, which have been explained by extended-chain crystallization.<sup>19</sup> Similar textures have been reported for anabarc polyethylene<sup>19,20</sup> and for 1,4-*trans*-polybutadiene<sup>21</sup> in the hexagonal columnar phase.

The different phases displayed by PDPeS and PDHS have been studied by means of temperature-dependent WAXS in the bulk state (Figure 6 and 7). Raising the temperature above the second disordering transition in the DSC heating thermograms yielded WAXS patterns with only a few features. The broad reflection centered around 20° (2 $\theta$ ) (4.45 Å) derives from the existence of poor periodicity between the mobile alkyl side groups. The main reflection at low angles corresponded to Bragg distances of 11.60 and 12.63 Å for PDPeS and PDHS,

**Figure 4.** Optical polarizing micrographs of poly(di-*n*-pentylsiloxane) upon cooling from the melt: (a) below the isotropization transition; (b) above the upper disordering transition; (c) in between the upper and the lower disordering transition.

respectively. For both materials, it was accompanied by a weak reflection at  $d/\sqrt{3}$ . Hence, it can be assumed that the polymer main chains are packed in a hexagonal columnar lattice. The broadness of the main reflection of PDHS at 300 K is due to overlap by a fraction of the high-temperature crystalline phase. The qualitatively similar appearance of the diffractograms of columnar mesomorphic PDES,<sup>3</sup> PDPeS, and PDHS confirms a similar type of local ordering of the polymer chains. Disappearance of all other sharp reflections upon transition



**Figure 5.** Optical polarizing micrographs of poly(di-*n*-hexylsiloxane) upon cooling from the melt: (a) below the isotropization transition; (b) above the upper disordering transition; (c) in between the upper and the lower disordering transition.

into the columnar mesophase indicates disordering of the side groups and long-range conformational disorder of the polymer main chain.

Further information about the thermal behavior of PDPeS and PDHS with regard to the mobility of the polysiloxane main chain in the different phases could be gained by measuring the  $^{29}\text{Si}$  chemical shift anisotropy ( $^{29}\text{Si}$  CSA).<sup>31-33</sup>

For PDES and PDPS it has been reported that fast conformational interconversion and diffusive rotation of the Si-O backbone segments as well as of the alkyl side chains is characteristic for the dynamically disordered  $\mu$ -phase.<sup>4,5</sup> As a consequence a motionally averaged axially symmetric  $^{29}\text{Si}$  CSA of 1.1 kHz has been observed, while the width of the CSA for the rigidity frozen molecules in the crystalline state at low temperatures was reported to be 3.1 kHz.

Figures 8 and 9 show the temperature dependence of the  $^{29}\text{Si}$  CSA of PDPeS and PDHS as observed upon heating. Axially symmetric signals with  $\nu_x' - \nu_z' = 1.0$  kHz

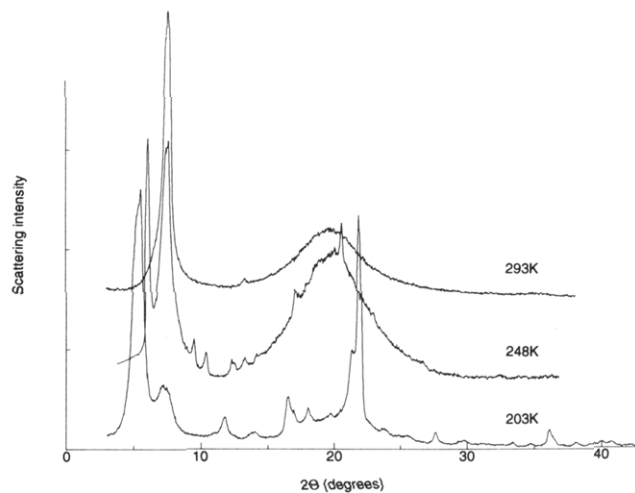


**Figure 6.** Temperature-dependent WAXS diffractograms of poly(di-*n*-pentylsiloxane). Temperature accuracy  $\pm 2$  K.

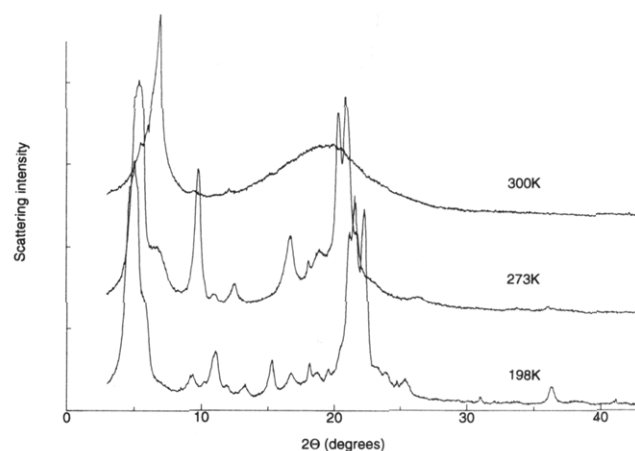


**Figure 7.** Temperature-dependent WAXS diffractograms of poly(di-*n*-hexylsiloxane). Temperature accuracy  $\pm 2$  K.

have been recorded 300 and 355 K, respectively, i.e., above the upper disordering transitions where the focal-conic fan texture was observed in the polarizing micrograph. Thus, also in the case of PDPeS and PDHS, the stepwise reduction of the CSA line width and the reversal of the main components of the chemical shift tensor before isotropization demonstrated the onset of diffusive bond rotation for the main-chain segments, similar to the  $\mu$ -phase of PDES,<sup>5,33</sup> PDPS,<sup>4,23</sup> and PDBS.<sup>4,23</sup> The observation of a similar motional state and of WAXS patterns corresponding to a hexagonal columnar lattice for all homologous poly(di-*n*-alkylsiloxane)s prepared so far demonstrates that they form the same type of a columnar (liquid crystalline) state as has been described for the  $\mu$ -phase of PDES and PDPS.<sup>1-5</sup>

Contrary to PDES and PDPS, no isotropic chemical shift signal could be observed superimposed to the  $\mu$ -phase  $^{29}\text{Si}$  CSA and PDPeS and PDHS, demonstrating that at ambient temperatures only a very small fraction of isotropic amorphous PDPeS and PDHS was present.

Corresponding to the results from the  $^{29}\text{Si}$  CSA experiments on PDHS and PDPeS, also the MAS  $^{29}\text{Si}$ -NMR experiments indicated a high segmental mobility in the mesomorphic state before isotropization. The temperature-dependent high-resolution MAS spectra of PDPeS and PDHS in parts a and b of Figure 10 show that only one sharp signal remained at  $-23.8$  ppm upon entering the  $\mu$ -phase above the upper disordering transition, belonging to the hexagonal columnar phase. The MAS  $^{29}\text{Si}$  NMR

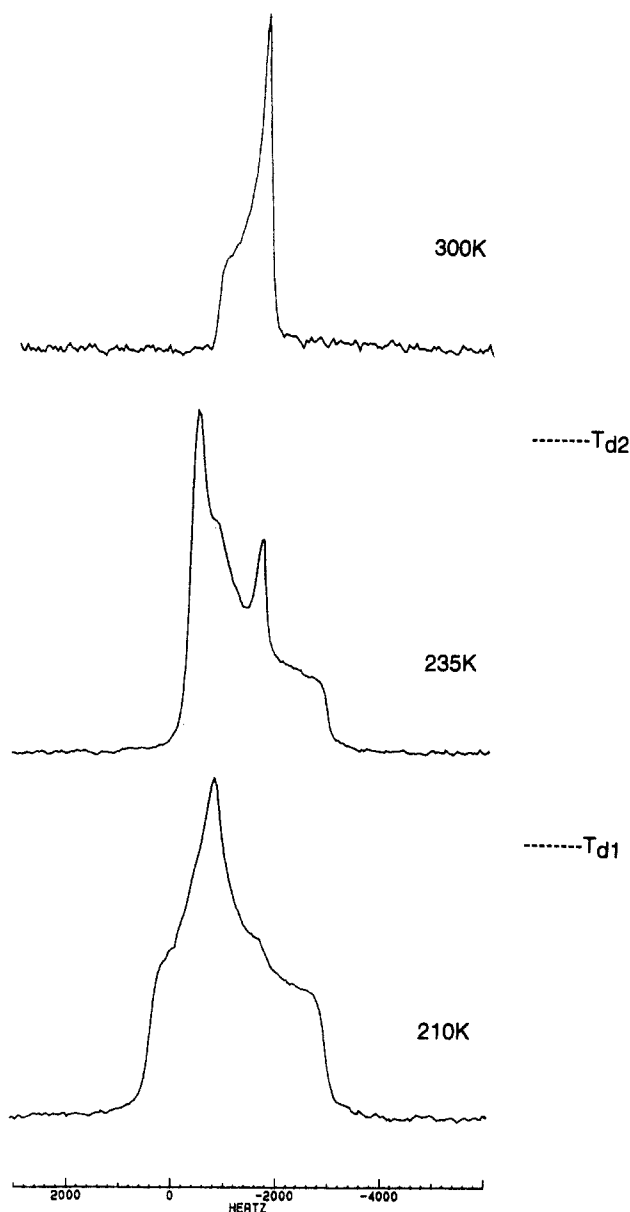


**Figure 8.** Temperature-dependent  $^{29}\text{Si}$  CSA of poly(di-*n*-pentylsiloxane). Temperature accuracy  $\pm 10$  K.

resonance is shifted upfield by 5 ppm compared to the signal assigned to the molecules in the low-temperature crystalline phase. Upfield shifts by several ppm are typically observed upon conformational disordering because of the increasing number of gauche conformations which contribute to the fast-exchange conformational equilibrium.<sup>31,32</sup>

Contrary to the observations reported above for PDPeS and PDHS, complete loss of the birefringence was observed in the microscopic studies on PDDS when the temperature was raised above the second transition observed in the DSC experiments. Correspondingly, no anisotropy of the chemical shift was observed when the  $^{29}\text{Si}$  NMR spectrum was recorded without magic angle spinning above 313 K (Figure 11). Apparently, PDDS is not able to form a hexagonal columnar  $\mu$ -phase and transforms at 313 K directly from a partially disordered crystalline phase into the isotropic melt. The MAS  $^{29}\text{Si}$  NMR spectrum in Figure 12 shows a similar upfield shift at the upper disordering transition as observed for PDPeS and PDHS. However, as the material is not anisotropically organized above this upper transition, the signal has to be assigned to the isotropic molten state. The similarity of the isotropic  $^{29}\text{Si}$  chemical shifts observed for the  $\mu$ -phase of PDPeS and

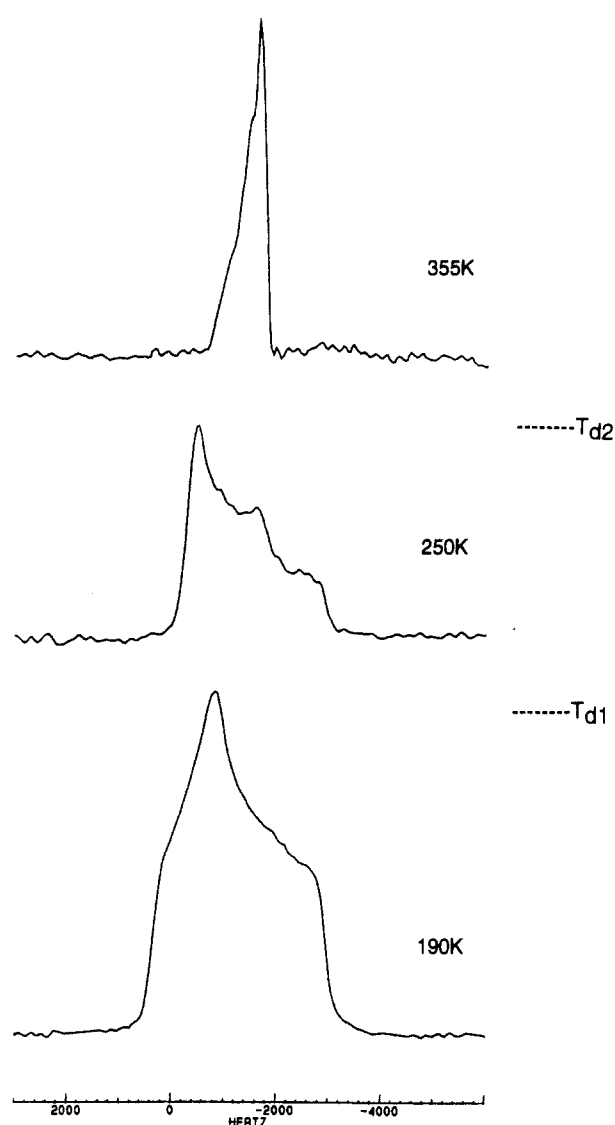


**Figure 9.** Temperature-dependent  $^{29}\text{Si}$  CSA of poly(di-*n*-hexylsiloxane). Temperature accuracy  $\pm 10$  K.

PDHS and for the isotropic state of PDDS clearly demonstrates the liquidlike character of the conformational interconversion in the hexagonal columnar phase.

**The Crystalline State.** Within the low-temperature crystalline phase of PDPeS and PDHS, the WAXS diffractograms showed a large number of sharp reflections, which pointed to a high degree of molecular order. A second feature was presented by the existence of a sharp and strong reflection at relatively small angles, corresponding to the interchain distance (Figures 6 and 7). Raising the temperature above the first disordering transition led to formation of the high-temperature crystal phase. Within this phase, the interchain reflection appeared to shift to wider angles and consequently to smaller Bragg distances (Figures 6 and 7). Furthermore, the number of sharp reflections decreased. As will be described below, the loss of periodicity can be explained by the onset of mobility of the side groups, which also causes the polymer main chain to gain limited mobility.

Additional and complementary information can be obtained from NMR studies on the  $^{29}\text{Si}$  CSA and the  $^{29}\text{Si}$  isotropic chemical shifts. The spectra allow us to follow segmental disordering, caused by the onset of particular molecular motions upon passing the first thermal transition. The CSA which has been observed for PDPeS at 210 K below the lower disordering transition (Figure 8) is nonaxially symmetric ( $\eta \approx 0.6$ ) with  $\nu_x - \nu_z = 3.5$  kHz. The

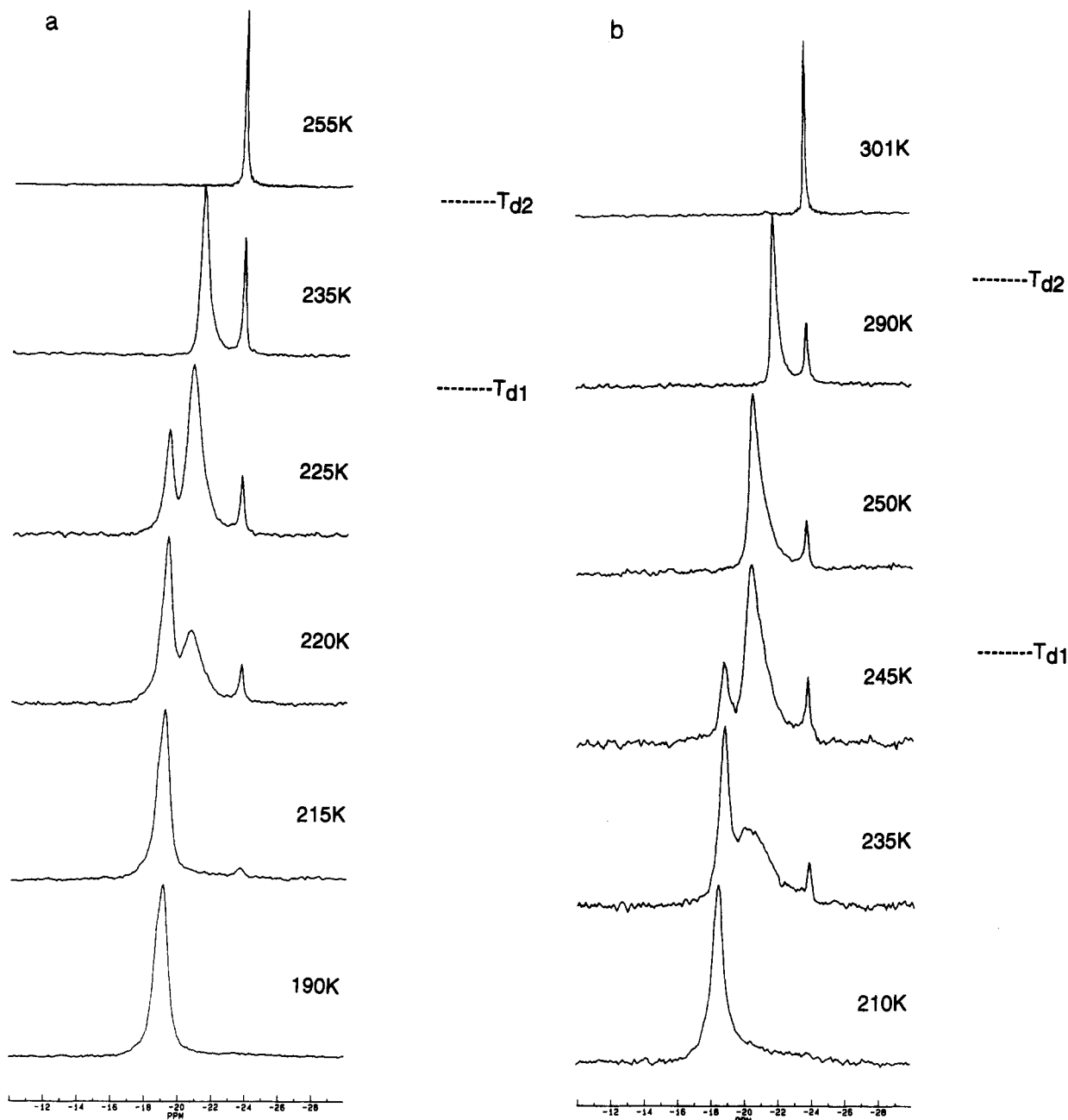


**Figure 10.** (a) Temperature-dependent MAS  $^{29}\text{Si}$  NMR spectra of poly(di-*n*-pentylsiloxane). Temperature accuracy  $\pm 10$  K. (b) Temperature-dependent MAS  $^{29}\text{Si}$  NMR spectra of poly(di-*n*-hexylsiloxane). Temperature accuracy  $\pm 10$  K.

broad signal is typical for the rigidly packed polysiloxane chain in the fully ordered low-temperature crystalline state. Raising the temperature above the first disordering transition to 235 K resulted in some motional averaging yielding a nearly axially symmetric CSA signal with  $\nu_x - \nu_z = 2.7$  kHz. In line with the results on PDES, the slight narrowing of the CSA line width can be explained by the onset of main-chain oscillations, caused by disordering of the side groups.<sup>5,33</sup> Furthermore, it can be noted that the  $^{29}\text{Si}$  CSA is overlapped by a narrow CSA signal belonging to a fraction of hexagonal columnar PDPeS.

The low-temperature  $^{29}\text{Si}$  CSA spectra of PDHS shown in Figure 9 are comparable to those of PDPeS with an apparently nonaxial CSA ( $\eta \approx 0.6$ ,  $\nu_x - \nu_z = 3.4$  kHz) at 190 K, an almost axially symmetric CSA for the high-temperature crystal phase ( $\eta \approx 0.1$ ,  $\nu_x - \nu_z = 2.7$  kHz) overlapped by the axially symmetric CSA ( $\nu_x' - \nu_z' = 1.0$  kHz) of a fraction of hexagonal columnar PDHS.

Consistent with the  $^{29}\text{Si}$  CSA spectra, the temperature dependence of the isotropic chemical shifts indicated the stepwise conformational disordering of the siloxane chains

correlated to the thermal transitions (Figure 10a,b). Below the first disordering transition, the spectra of both PDPeS and PDHS showed only one relatively broad signal at -19 and -18.7 ppm, respectively. Likewise, PDDS showed a resonance signal at -18.7 ppm in the low-temperature crystalline phase, but the presence of a broad signal located slightly upfield revealed that not all material was neatly crystallized within this phase and remained present as a fraction of undercooled material.

Raising the temperature above  $T_{d1}$  resulted in a rather narrow fast-exchange MAS  $^{29}\text{Si}$  signal at -20 ppm for both PDPeS and PDHS, indicating a similar averaged main-chain conformation in the high-temperature crystalline phase. For both compounds, this signal shifted upfield with increasing temperature to -21.2 and -21.8 ppm for PDPeS and PDHS, respectively. Furthermore, a significant fraction of hexagonal columnar material was indicated by the appearance of a signal at -23.8 ppm.

For PDDS, formation of the -22 ppm signal of the molecules in the high-temperature crystalline phase is preceded by the occurrence of a signal at -23.8 ppm (Figure



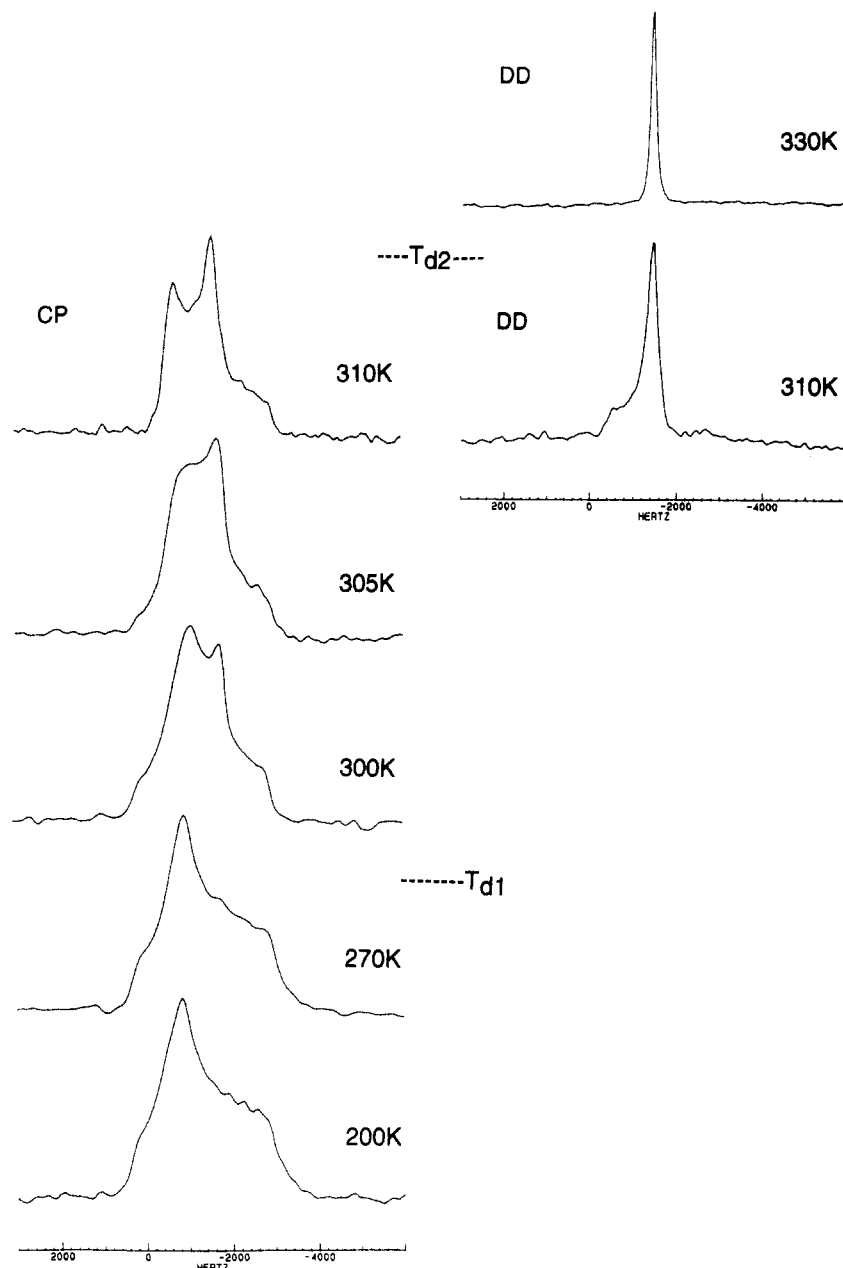


**Figure 11.** Temperature-dependent  $^{29}\text{Si}$  CSA of poly(di-*n*-decylsiloxane). CP: recorded with cross-polarization in combination with dipolar decoupling. DD: recorded without cross-polarization. Temperature accuracy  $\pm 10$  K.

12; spectrum at 290 K). A gradual narrowing of the  $^{29}\text{Si}$  CSA was observed at the lower disordering transition upon heating (Figure 11). The nonaxially symmetric CSA with  $\nu_x - \nu_z = 3.4$  kHz at 200 K transformed slowly into an axially symmetric CSA with  $\nu_x - \nu_z = 2.7$  kHz at 310 K, characteristic of the high-temperature crystalline phase. This indicates a gradual increase of motional freedom and is consistent with the broad thermal effect noted in the DSC heating thermogram (Figure 3). The still relatively broad CSA above  $T_{d1}$  appeared to be overlapped by a narrower axially symmetric CSA. This became obvious when the CSA was recorded without cross-polarization. In this case, the slower relaxing crystalline phase was not detected and only a narrow axially symmetric CSA remained with  $\nu_x - \nu_z = 1.3$  kHz. Further heating to 330 K yielded the narrow isotropic signal of the PDDS melt.

In agreement with the observation of a MAS signal at  $-23.8$  ppm, the narrowed CSA component at 270–310 K indicated formation of an undercooled mesomorphic fraction. Thus also PDDS seems to be able to form a highly mobile anisotropic  $\mu$ -phase like has been observed for the lower poly(di-*n*-alkylsiloxane)s. However, whereas

the  $\mu$ -phase is thermodynamically favored for PDPeS and PDHS within the appropriate temperature regime, it is only observed as a metastable modification for PDDS.

In order to address the thermodynamic stability of the phases in further detail, the three polysiloxanes have been studied further by means of annealing and quenching experiments. Annealing PDPeS at 250 and 225 K did not yield a change in the DSC signal intensity, which indicated that both transitions belonged to the same modification. Upon cooling PDPeS from room temperature to 193 K at a rate of 5 K/min, only one crystallization transition was observed at 227 K, but reducing the rate to 0.5 K/min allowed us to resolve two separate transitions at 222 and 227 K (Figure 13). The hysteresis was larger for the upper disordering transition than for the lower one. This can be explained by the higher degree of molecular disorder in the hexagonal columnar phase compared to the high-temperature crystalline phase.

Figure 14 shows a DSC diagram obtained from a PDPeS sample which had been quenched from the hexagonal columnar  $\mu$ -phase at 323 K, to 77 K. Apart from the glass transition (a) at 167 K, two recrystallization peaks could

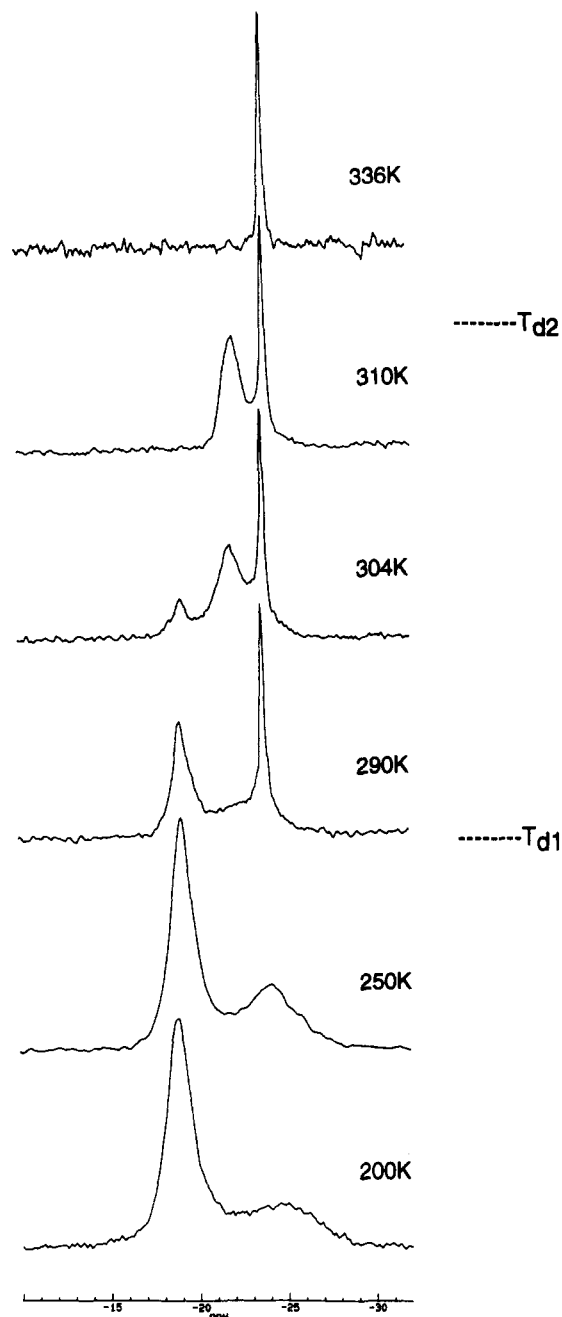


**Figure 12.** Temperature-dependent MAS  $^{29}\text{Si}$  NMR spectra of poly(di-*n*-decylsiloxane). Temperature accuracy  $\pm 10$  K.

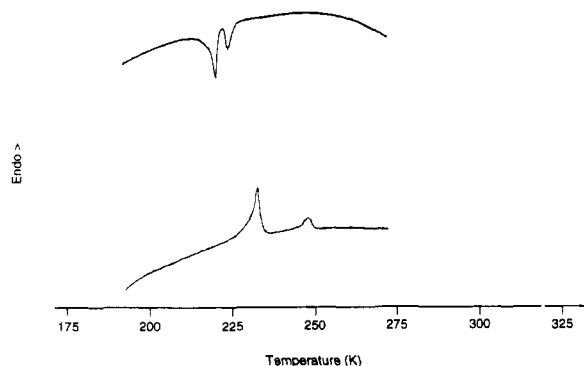


**Figure 13.** DSC heating and cooling scan of poly(di-*n*-pentylsiloxane) (rate 0.5 K/min).

be discerned with approximate onset temperatures at 183 (b) and 203 K (c). Further heating yielded the two disordering transitions (d and e) described before. In view of the fact that the isotropization transition of PDPeS is at 603 K and that the isotropic fraction at room tem-

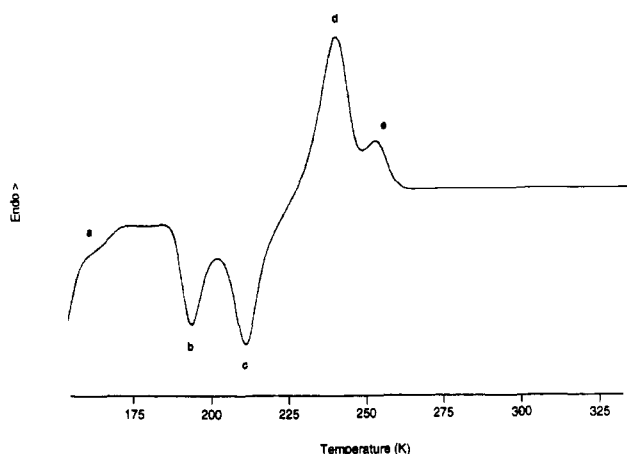


**Figure 14.** DSC heating scan of poly(di-*n*-pentylsiloxane) after quenching from 323 to 77 K (rate 20 K/min).

perature is small according to NMR and birefringence, it appears improbable that the first recrystallization peak (b), with its significant transition enthalpy, is due to a fraction of vitrified amorphous material. Moreover, as the sum of the transition enthalpies of the two recrystallizations b and c is comparable to that of the two disordering transitions d and e, it seems likely that the two transitions are due to the vitrification of a fraction of the  $\mu$ -phase and a fraction of the partially disordered crystalline state. Thus, the two recrystallization peaks might be seen as an indication of two types of a mesoglass differing in the amount of disorder present in the polymer main chain. Similar double recrystallization peaks have been reported before the PDPS and PDBS and had been explained by the coexistence of an amorphous glassy fraction and a mesomorphic glassy fraction.<sup>4</sup>

Upon cooling PDHS at a rate of 5 K/min from the hexagonal columnar mesophase to 193 K, two well-resolved crystallization transitions are observed at 248 and 277 K (Figure 2). Like in case of PDPeS (Figure 1), the larger disorder in the columnar mesophase is reflected in a larger hysteresis effect for the upper disordering transition compared to the lower one. Neither variation in cooling rates nor annealing experiments in between the two transitions and below the lower transition yielded significant changes in transition enthalpies or temperatures. In the case of lower molecular weight samples of PDHS ( $M_w \leq 180\,000$ ), a weak third transition was observed at 284 K upon heating, which could not be correlated to conformational changes by means of  $^{29}\text{Si}$  NMR.

In contrast to PDPS, PDBS, and PDPeS, quenching a PDHS sample from 473 to 77 K did not allow us to observe a glass transition or any recrystallization effects. Apparently, crystallization of PDHS is extremely fast.

Only one transition could be observed at 303 K upon cooling PDDS (Figure 3). Neither annealing below the lower transition or in between the two transitions nor variation of cooling rates yielded a significant change of the DSC thermograms. Like in the case of PDHS, quenching a sample from the isotropic melt at 333 to 77 K did not allow us to observe a glass transition during the subsequent heating scan.

## Conclusions

Three new poly(di-*n*-alkylsiloxane)s have been synthesized and characterized with respect to their thermal behavior. Like the lower homologues, all three compounds exhibit two disordering transitions before isotropization. Below  $T_{d1}$ , the phase state can be described as rigid crystalline, the  $^{29}\text{Si}$  CSA being nonaxially symmetric with



$\nu_x - \nu_z = 3.4$  kHz. Upon heating above  $T_{d1}$ , a high-temperature crystalline phase was formed, characterized by a decrease in the  $^{29}\text{Si}$  CSA which is explained by the onset of small backbone librations and by disordering of the side groups.

Above the upper disordering transition  $T_{d2}$ , PDPeS and PDHS form similar hexagonal columnar mesophases, characterized by complete conformational disordering of the polymer main chain and the side groups.

If the polysiloxanes are symmetrically substituted by *n*-butyl, *n*-pentyl, or *n*-hexyl side groups, this  $\mu$ -phase appears to be remarkably stable and can be observed over a temperature interval of 300–350 K. PDDS, however, is not able to form a stable columnar mesophase. The stabilization of the columnar state by longer side groups appears to be overruled at a certain length of the alkyl substituents. It seems likely that, in the case of long alkyl substituents, the packing and the segmental motion of the main chain and the side groups become more and more decoupled. In other words, side-chain crystallization can occur without ordering of the polymer backbone.<sup>34</sup> As the difference in entropy between the two-dimensionally ordered columnar mesophase of poly(di-*n*-alkylsiloxane)s and the isotropic melt is very small because of the large amount of conformational disorder present in the mesophase, it is clear that mesophase formation is easily hindered by any competitive ordering process.

Coexistence of the columnar mesophase and the high-temperature crystalline phase appears to be a common feature of the melting behavior of poly(di-*n*-alkylsiloxane)s. The presence of a hexagonal columnar fraction aside the high-temperature crystalline phase might be explained either by a structural heterogeneity of the molecules due to the relatively broad molecular weight distribution and the eventually present large ring molecules of the poly(di-*n*-alkylsiloxane)s or also by topological constraints such as trapped entanglements which hinder crystallization but which can still be incorporated within the hexagonal columnar order. The observation that PDDS is only able to exhibit a columnar mesophase in conjunction with the high-temperature crystalline phase indicates that the crystalline framework might support mesomorphic ordering, e.g., of rather densely packed molecules or molecular segments on top of crystalline lamellae like in the fringed micelle model.

## References and Notes

- (1) Lee, C. L.; Johansson, O. K.; Flanigan, O. L.; Hahn, P. *Polym. Prepr. (Am. Chem. Soc., Div. Polym. Chem.)* **1969**, *10* (2), 1311.
- (2) Beatty, C. L.; Pochan, J. M.; Froix, M. F.; Hinman, D. D. *Macromolecules* **1975**, *8*, 547.
- (3) Godovsky, Yu. K.; Papkov, V. S. *Adv. Polym. Sci.* **1989**, *88*, 129.
- (4) Möller, M.; Siffrin, S.; Kögler, G.; Oelfin, D. *Makromol. Chem., Macromol. Symp.* **1990**, *34*, 171.
- (5) Kögler, G.; Loufakis, K.; Möller, M. *Polymer* **1990**, *31*, 1538.
- (6) Miller, R. D.; Michl, J. *Chem. Rev.* **1989**, *89*, 1359.
- (7) Schilling, F. C.; Bovey, F. A.; Lovinger, A. J.; Zeigler, J. M. *Adv. Chem. Ser.* **1990**, *224*, 341.
- (8) Karikari, E. K.; Greso, A. J.; Farmer, B. L.; Miller, R. D.; Rabolt, J. F. *Macromolecules* **1993**, *26*, 3937.
- (9) Tur, D. R.; Provotorova, N. P.; Vinogradova, S. V.; Bakhmutov, V. I.; Galakhov, M. V.; Zhukov, V. P.; Dubovik, I. I.; Tsvankin, D. Ja.; Papkov, V. S. *Makromol. Chem.* **1991**, *192*, 1905.
- (10) Papkov, V. S.; Il'ina, M. N.; Zhukov, V. P.; Tsvankin, D. Ja.; Tur, D. R. *Macromolecules* **1992**, *25*, 2033.
- (11) Cotts, P. M.; Miller, R. D.; Trefonas, P. T., III; West, R.; Fickes, G. N. *Macromolecules* **1987**, *20*, 1046.
- (12) Cotts, P. M.; Ferline, S.; Dagli, G.; Pearson, D. S. *Macromolecules* **1991**, *24*, 6730.
- (13) Mark, J. E.; Chiu, D. S.; Su, T.-K. *Polymer* **1978**, *19*, 407.
- (14) Papkov, V. S.; Svistunov, V. S.; Godovsky, Yu. K.; Zhdanov, A. A. *J. Polym. Sci., Polym. Phys.* **1987**, *25*, 1859.
- (15) Petersen, D. R.; Carter, D. R.; Lee, C. L. *J. Macromol. Sci., Phys.* **1969**, *B3* (3), 519.
- (16) Frey, H. H. *Structure, Organization and Function of Polysilylene Copolymers*. Ph.D. Thesis, University of Twente, Enschede, The Netherlands, 1993, p 134.
- (17) Weber, P.; Guillon, D.; Skoulios, A.; Miller, R. D. *J. Phys. Fr.* **1989**, *50*, 793.
- (18) Wunderlich, B.; Möller, M.; Grebowicz, J.; Baur, H. *Adv. Polym. Sci.* **1988**, *87*, 1.
- (19) Hikosaka, M.; Rastogi, S.; Keller, A.; Kawabata, H. *J. Macromol. Sci., Phys.* **1992**, *B31* (1), 87.
- (20) Basset, D. C. *Principles of Polymer Morphology*; Cambridge University Press: Cambridge, U.K., 1981.
- (21) Rastogi, S.; Ungar, G. *Macromolecules* **1992**, *25*, 1445.
- (22) Ungar, G. *Polymer* **1993**, *34*, 2050.
- (23) Siffrin, S. In *Cyclo- and Poly(di-*n*-alkylsiloxane)s with Ethyl, Propyl and Butyl Side Groups*. Ph.D. Thesis, University of Twente, Enschede, The Netherlands, 1993.
- (24) Benoit, H.; Rempp, R.; Grubisic, Z. *J. Polym. Sci.* **1967**, *B5*, 753.
- (25) Sanayei, R. A.; Pang, S.; Rudin, A. *Polymer* **1993**, *34*, 2320.
- (26) Takiguchi, T.; Sakurai, M.; Kishi, T.; Ichimura, J.; Iizuka, Y. *J. Org. Chem.* **1960**, *25*, 310.
- (27) Out, G. J. J.; Klok, H. A.; Schwegler, L.; Frey, H.; Möller, M., submitted to *Makromol. Chem.*
- (28) Out, G. J. J.; Klok, H. A.; Möller, M., submitted to *Makromol. Chem.*
- (29) Varma-Nair, M.; Wesson, J. P.; Wunderlich, B. *J. Thermal Anal.* **1989**, *35*, 1913.
- (30) Miller, K. J.; Grebowicz, J.; Wesson, J. P.; Wunderlich, B. *Macromolecules* **1990**, *23*, 849.
- (31) Möller, M. *Adv. Polym. Sci.* **1985**, *66*, 59.
- (32) Tonelli, A. E. *NMR Spectroscopy and Polymer Microstructure, The Conformational Connection*; VCH Publishers, Inc.: New York, 1989.
- (33) Litvinov, V. M.; Whittacker, A. K.; Hagemeyer, A.; Spiess, H. W. *Colloid Polym. Sci.* **1989**, *267*, 681.
- (34) Plate, N. A.; Shibaev, V. P. In *Comb-like polymers and liquid crystals*; Plenum Press: New York, 1987.